Supplement of Atmos. Chem. Phys., 23, 15491–15505, 2023
https://doi.org/10.5194/acp-23-15491-2023-supplement

Atmospheric Chemistry and Physics
Open Access
EGU

Supplement of

The impact of ENSO and NAO initial conditions and anomalies on the modeled response to Pinatubo-sized volcanic forcing

Helen Weierbach et al.

Correspondence to: Kostas Tsigaridis (kostas.tsigaridis@columbia.edu)

Introduction Additional diagnostics and information for the GISS VolMIP simulations used in this analysis. First, we present a histogram of ENSO and NAO conditions under both control and perturbed conditions for the VolMIP and random samples presented in the main text (Figure S1). We also present common metrics related to the radiative forcing response (Figure S2) and the surface temperature response globally and in the tropics across different ensemble groups (Figure S4). Finally we also present additional metrics to supplement the main results in the main text: in particular we present the relative sea surface temperature response for El Nino Southern Oscillation (Figure S4) and the mean response for sampled NAO groups for eastward winds at 500mb.

1 Additional Results

Figure S1 supplements information from Figure 1 to show how the distribution of the ENSO and NAO indices change in the first winter of the selected simulation year for both VolMIP samples (n=81) and Random samples (n=50) under volcanic perturbations.

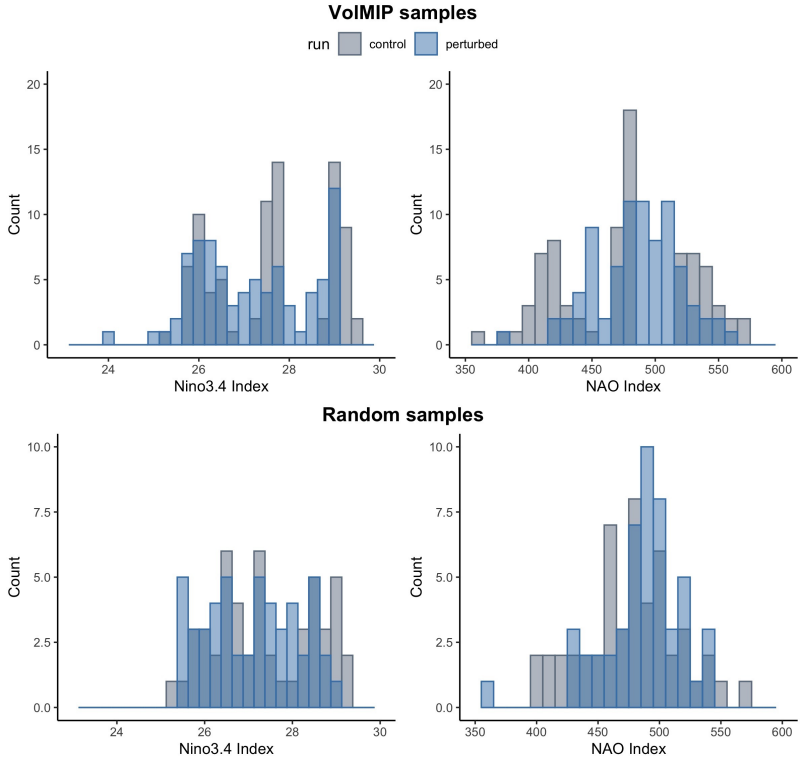

Figure. S1. Histogram of control(grey) and perturbed(blue) ENSO and NAO conditions for both VolMIP samples (top) and random samples (bottom).

1.1 Radiative Forcing

Prescribed volcanic sulfate aerosols in the stratosphere cause changes in shortwave and longwave radiative forcing by reflecting solar radiation and absorbing infrared radiation. These affects are measured by changes in incoming and outgoing radiation at the surface and top of atmosphere. Beginning the month of the eruption, global shortwave radiation reaching Earth's surface decreases, with ensemble mean forcing peaking at -3.27 W m^{-2} the December after the eruption. This magnitude of

volcanic radiative flux is in good agreement with both other model studies and satellite-based observations (Schmidt et al., 2018). Changes in shortwave forcing at the top of the atmosphere shows an almost identical pattern with decreases peaking in December at -3.83 W m^{-2}. Ensembles also show changes in longwave radiative forcing at the top of the atmosphere with an increase in longwave forcing at the top of the atmosphere beginning on the first October after the eruption, lasting consistently for one year and decaying after the second fall. Longwave impacts lag behind shortwave forcing, with a peak occurring the July after the eruption with a magnitude of 1.64 $\frac{W}{m^2}$. There is minimal variation in the observed radiative forcing response between ensembles, indicating that such responses are not significantly impacted by background conditions. At peak forcing the composite of 81 simulations have a standard deviation of only 0.020 $\frac{W}{m^2}$ for shortwave forcing at the surface and 0.0010 $\frac{W}{m^2}$ for longwave forcing at the top of the atmosphere. Shortwave and longwave radiative impacts for volcanic sulfate aerosols are presented in S2 where all radiative forcing impacts are presented at the surface and top of the atmosphere.

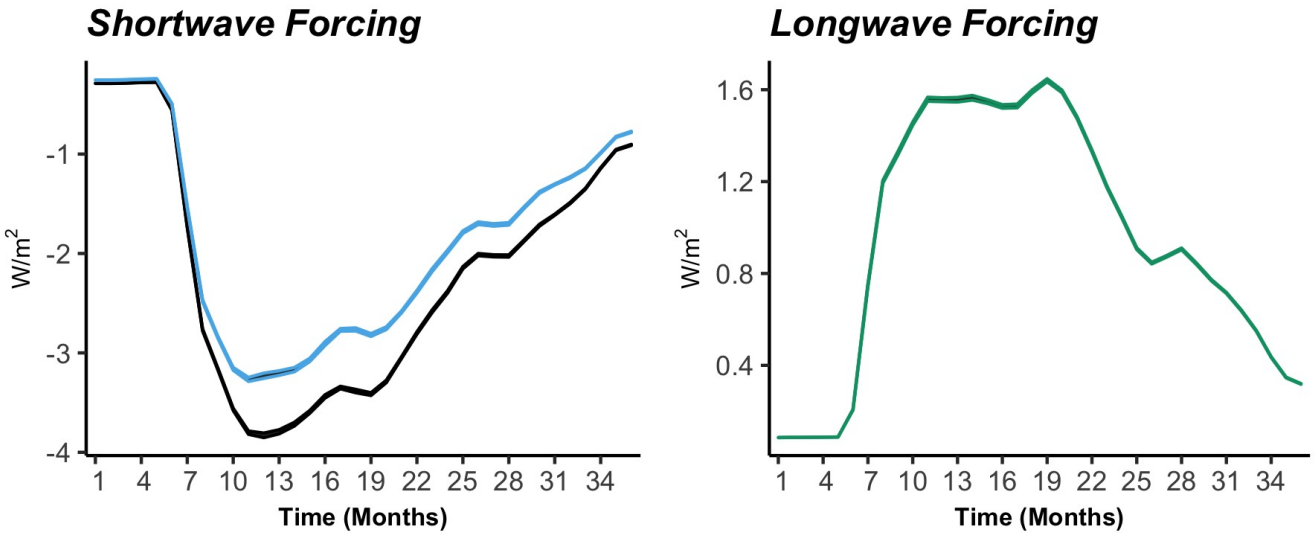

Figure. S2. 3-year time series of global shortwave radiative forcing (left) at the surface (light blue) and top of atmosphere (black). Longwave radiative forcing at the top of atmosphere (green). Each line is shaded with one standard deviation for all 81 ensembles above and below the mean response. For each ensemble the volcanic eruption occurs in the 6th month.

1.2 Surface Temperature

Global surface temperature decreases the first year after the eruption with an anomaly peaking at a -0.35°C the first spring after the eruption. Ensemble groups with different initial ENSO phases show some variability in the mean global surface temperature response to volcanic eruptions. These differences between ensemble groups are, however within the ensemble variations (Figure S3). The tropical [20 °S - 20 °N] surface temperature reduction is stronger than the global mean surface temperature response, with an ensemble average decrease of -0.43 °C. Tropical surface temperature anomalies also vary between different initial conditions, particularly in the first winter. Surface air temperature in the tropics decreases by an average of 0.2 degrees mores in positive and neutral ENSO simulations than in negative ENSO simulations (Figure S3). This variability between negative ENSO groups compared to other ensembles is significant for the first 7-13 months after the eruption as verified by a pairwise comparison ANOVA test (an analysis technique which verifies the statistical variance between two groups).

Neither global nor tropical surface temperature re-equilibrate to normal conditions (anomaly of zero) before the end of the 3-year simulation due to the high thermal capacity of the ocean. This is expected as global temperature effects can take as long as a decade to return to normal (Stenchikov et al., 1998). Here we instead focus on the regional climate impacts on the

inter-annual time scale. Initial NAO conditions cause no large scale variations in the surface temperature response and thus are not pictured. The influence of NAO initial conditions on regional scale surface temperature is further discussed in Sect. 3.4.3.

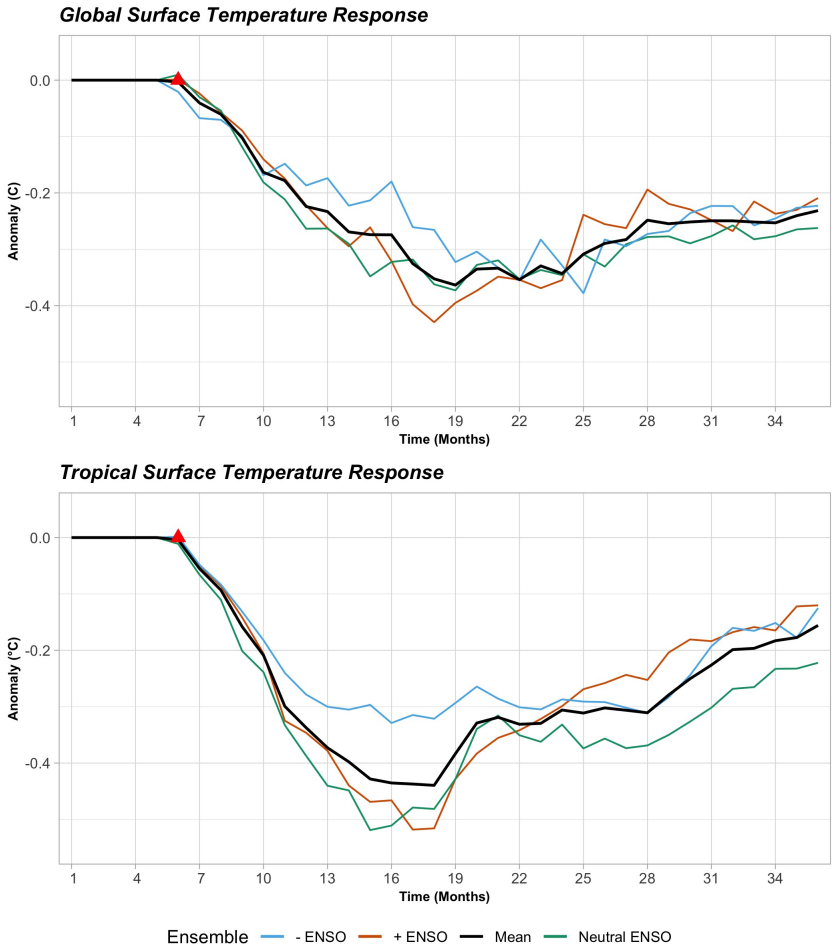

Figure. S3. Anomalous global (top) and tropical [20°S- 20°N] (bottom) temperature response for ensembles varying by initial ENSO condition. Negative ENSO simulations (blue) have weaker surface cooling, particularly in the tropics, during the first post-eruptive spring. Positive and neutral ensembles have similar surface cooling at both the global and tropical scale.

1.3 Supplemental Metrics

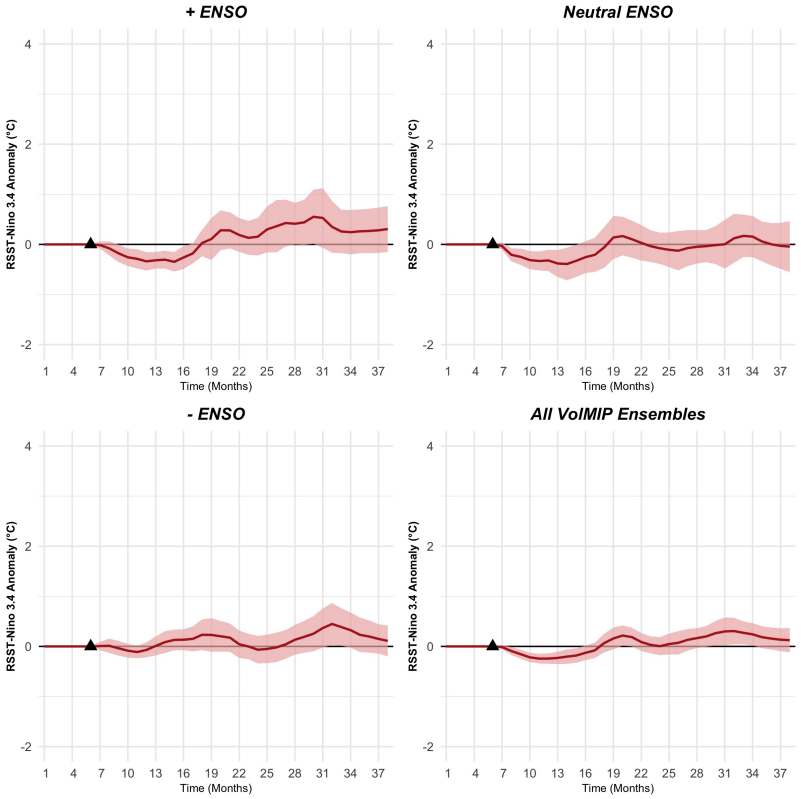

Figure. S4. The response of the relative sea surface temperature response in the El Niño 3.4 region (see Khodri et al. (2017), for positive, neutral, and negative ENSO ensemble groups, and for all VolMIP ensembles.

References

Khodri, M., Izumo, T., Vialard, J., Janicot, S., Cassou, C., Lengaigne, M., Mignot, J., Gastineau, G., Guilyardi, E., Lebas, N., et al.: Tropical explosive volcanic eruptions can trigger El Niño by cooling tropical Africa, Nature communications, 8, 1–13, 2017.

Schmidt, A., Mills, M. J., Ghan, S., Gregory, J. M., Allan, R. P., Andrews, T., Bardeen, C. G., Conley, A., Forster, P. M., Gettelman, A., et al.: Volcanic radiative forcing from 1979 to 2015, Journal of Geophysical Research: Atmospheres, 123, 12 491–12 508, 2018.

Stenchikov, G., Kirchner, I., Robock, A., Graf, H.-F., Antuña, J. C., Grainger, R. G., Lambert, A., and Thomason, L.: Radiative forcing from the 1991 Mount Pinatubo volcanic eruption, Journal of Geophysical Research: Atmospheres, 103, 13 837–13 857, 1998.

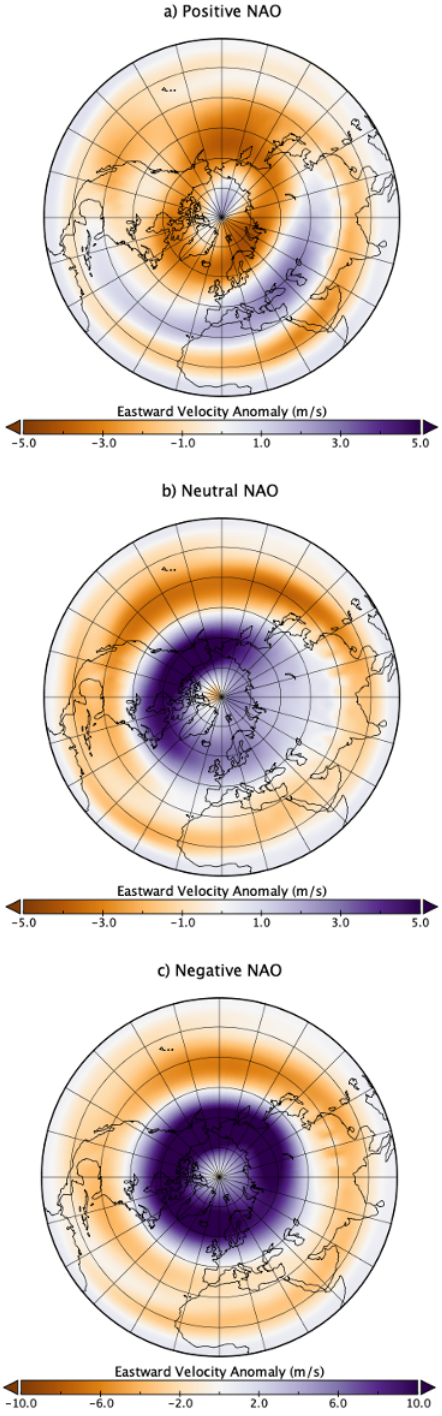

Figure. S5. The mean anomalous response of eastward velocity for each VolMIP NAO group in the first winter (December-February mean.)